Received December 1997

An energy-transport model for semiconductor heterostructure devices: application to AlGaAs/GaAs MODFETs

Cédric Lab and Philippe Caussignac
Département de mathématiques,
Ecole polytechnique fédérale de Lausanne, Switzerland

Keywords *Energy-transport, Finite element, Semiconductors, Simulation, Transport*

Abstract *A stationary 3D energy-transport model valid for semiconductor heterostructure devices is derived from a semiclassical Boltzmann equation by the moment method. In addition to the well-known conservation equations, we obtain original interface conditions, which are essential to have a mathematically well-posed problem. An appropriate modelling of the physical parameters appearing in the system of equations is proposed for gallium arsenide. The model being written and its particularities mentioned, we present a novel numerical algorithm to solve it. The discretization of the equations is achieved by means of standard and mixed finite element methods. We apply the model and numerical algorithm to simulate a 2D AlGaAs/GaAs MODFET. Comparisons between experimental measurements and calculations are carried out. The influence of the modelling of the physical parameters, especially the electron mobility and the energy relaxation time, is noted. The results show the satisfactory behaviour of our model and numerical algorithm when applied to GaAs heterostructure devices.*

Introduction

For the last decade, numerical simulation of semiconductor devices has evolved a lot. The main efforts have been applied to homogeneous semiconductor devices, particularly to those based on silicon technology (MOSFETs). The models used for these simulations are various and extend from kinetic to drift-diffusion ones (see Markovich *et al.,* 1991). In contrast with drift-diffusion equations, hydrodynamic or energy-transport models have not been thoroughly studied, especially in the case of non-homogeneous semiconductors. Thus, the first aim of our work is to extend such models to heterostructure devices. We therefore derive interface conditions and obtain an energy-transport model suitable for the simulation of heterostructure devices. We notice that our interface conditions correspond to those obtained in Poupaud and Yamnahakki (1990). The second goal of the present work is to propose novel numerical methods to solve the above-mentioned model. On the contrary to most methods that can be found in the literature, in which finite volumes (Forghieri *et al.,* 1988; SILVACO International, 1995; Technology Modeling Associates, 1994) or finite differences (Feng and Hintz, 1988; Shawki, 1990; Snowden and Loret, 1987) are used to discretize the equations, we employ standard and mixed triangular finite elements. As mentioned in El Boukili (1995), this kind of discretization allows a greater flexibility, in the

 © MCB University Press, 0332-1649

sense that complicated device geometries can be simulated with the help of locally unstructured meshes.

The paper is organized as follows. In the next section, we derive an energy-transport model suitable for the simulation of heterostructure devices from a semiclassical Boltzmann equation, paying special attention to interface conditions. Boundary conditions for the system of equations are proposed. The modelling of the physical parameters for the case of gallium arsenide is studied thereafter. The following section describes the numerical methods used to solve the system of equations. The mathematical formulation of the model is emphasized, the decoupling scheme and the discretization methods are given. Finally, we validate the model and the numerical methods on a 2D AlGaAs/GaAs MODFET. Examples of results are shown and compared to experimental measurements whenever possible. To conclude, the influence of the model and of the physical parameters is discussed.

Physical model

We consider a semiconductor heterostructure device $\Omega \subset R^3$ composed of M semiconductors Ω_i separated from each other by N abrupt interfaces $\Gamma_j(\overline{\Omega} = \cup_{i=1}^{M} \overline{\Omega}_i$, see Figure 1).

On these interfaces, the electron affinity χ, the electron effective mass m and the semiconductor dielectric constant ϵ are discontinuous. The boundary $\partial\Omega$ of the device is made of three disjoint parts $\partial\Omega_O$, $\partial\Omega_S$ and $\partial\Omega_N$. The part $\partial\Omega_O$ corresponds to ohmic contacts, $\partial\Omega_S$ to Schottky contacts and $\partial\Omega_N$ to interfaces with insulating materials. Our aim is to describe the electron transport in such a device by means of a semiclassical macroscopic model. In each Ω_i, $i = 1, 2, \dots, M$, where χ and m are assumed sufficiently smooth functions of the position, the electron transport can be described by the Boltzmann equation:

$$\partial_t f + \nabla_{\boldsymbol{x}} f \cdot \nabla_{\boldsymbol{p}} H - \nabla_{\boldsymbol{p}} f \cdot \nabla_{\boldsymbol{x}} H = Q(f), \tag{1}$$

where H is the Hamiltonian of the electron, given by (see Marshak and van Vliet, 1984):

$$H(\boldsymbol{x}, \boldsymbol{p}, t) = \frac{|\boldsymbol{p}|^2}{2m(\boldsymbol{x})} - (q\phi(\boldsymbol{x}, t) + \chi(\boldsymbol{x})). \tag{2}$$

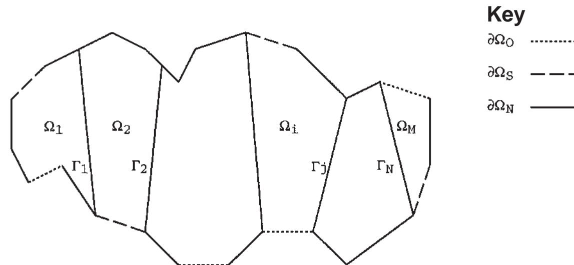

Figure 1.
Sketch of a semiconductor heterostructure device

In equations (1) and (2), t is the time, $\boldsymbol{x}$ the position, $\boldsymbol{p}$ the momentum, f the electron distribution function, $Q(f)$ a collision operator describing the interactions between the electrons and the crystal lattice, ϕ the electric potential. We insert (2) in (1) and get the following Boltzmann equation:

$$\partial_t f + \frac{\boldsymbol{p}}{m}\nabla_{\boldsymbol{x}} f - \left[\frac{1}{2}|\boldsymbol{p}|^2 \nabla_{\boldsymbol{x}}\left(\frac{1}{m}\right) - \nabla_{\boldsymbol{x}}(q\phi + \chi)\right] \cdot \nabla_{\boldsymbol{p}} f = Q(f). \tag{3}$$

To connect the microscopic description of the electron gas given by equation (3) with its macroscopic dynamics, we apply the well-known moment method. Following the procedure described in Cercignani (1990), we multiply equation (3) by $1, \boldsymbol{p}, |\boldsymbol{p}|^2$ and integrate it over the momentum space. We obtain a set of three conservation equations for the macroscopic quantities that characterize the electron gas: electron density, momentum and energy. At this stage, two problems remain: the system of equations is not closed (more unknowns than equations) and the integrals of the collision operator cannot be expressed as functions of the macroscopic quantities. To solve the first problem, we introduce the usual phenomenological closure relations: the stress tensor is diagonal, proportional to the scalar electron temperature, and the heat flux is given by a Fourier law. To get rid of the second problem, integrals of the collision operator are expressed with relaxation time approximations (see Baccarani and Wordeman, 1985). To obtain a stationary system suitable for heterostructures, we suppress the time dependent terms in the equations and neglect the convective term in the momentum conservation equation. This term indeed prevents from writing jump conditions at the interface between two different semiconductors. Its suppression is partly justified by the work of Poupaud and Yamnahakki (see Poupaud and Yamnahakki, 1990) and its influence in a hydrodynamic model is quantized in Feng and Hintz (1988). We obtain the following set of equations:

$$\boldsymbol{J} = k\mu T\nabla n + k\mu n\nabla T - \mu n\nabla(q\phi + \chi) - \frac{3}{2}k\mu nT\nabla \ln m, \tag{4}$$

$$\nabla \cdot \boldsymbol{J} = 0, \tag{5}$$

$$\boldsymbol{S} = -\frac{1}{q}\left(\frac{m}{2q^2}\frac{|\boldsymbol{J}|^2}{n^2} + \frac{5}{2}kT\right)\boldsymbol{J} - \kappa\nabla T, \tag{6}$$

$$\nabla \cdot \boldsymbol{S} = -\boldsymbol{J} \cdot \nabla\left(\phi + \frac{\chi}{q}\right) - \frac{n}{\tau_w}\left[\frac{m}{2q^2}\frac{|\boldsymbol{J}|^2}{n^2} + \frac{3}{2}k(T - T_0)\right]. \tag{7}$$

The system has to be coupled to the Poisson equation, that links the electron density to the scalar electric potential:

$$-\nabla \cdot (\epsilon\nabla\phi) = q(N_d^+ - n). \tag{8}$$

In equations (4) to (8), the unknowns are the electron density n, the electron temperature T and the scalar electric potential ϕ. The parameter k is the Boltzmann constant, q is the positive elementary charge, χ is the electron affinity, m is the electron effective mass, ϵ is the semiconductor dielectric constant, μ is the electron mobility, τ_w is the energy relaxation time, T_0 is the lattice temperature, N_d^+ is the ionized donor density, $\boldsymbol{J}$ is the current density and $\boldsymbol{S}$ is the energy flux density.

The set of nonlinear tightly coupled partial differential equations (4) to (8) is valid in each semiconductor Ω_i, $i = 1, 2, \ldots, M$. To obtain a system defined everywhere on Ω, it is necessary to complete it with appropriate jump conditions on interfaces Γ_j, $j = 1, 2, \ldots, N$. With this aim, we notice that equations (5), (7) and (8) are in the conservative form, so that we must impose the continuity of the normal component of $\boldsymbol{J}$, $\boldsymbol{S}$ and $\boldsymbol{D} = \epsilon \nabla \phi$ on each interface. Thus, denoting by $[.]_{\Gamma_j}$ the jump of a quantity across Γ_j and ν the unit normal to the interface, we set ($j = 1, 2, \ldots, N$):

$$[\boldsymbol{J} \cdot \nu]_{\Gamma_j} = 0, \tag{9}$$

$$[\boldsymbol{S} \cdot \nu]_{\Gamma_j} = 0, \tag{10}$$

$$[\epsilon \nabla \phi \cdot \nu]_{\Gamma_j} = 0. \tag{11}$$

As $\boldsymbol{J}$, $\boldsymbol{S}$ and $\boldsymbol{D}$ depend on the gradient of quantities, we have to impose the continuity of these quantities at interfaces, and we therefore have:

$$[T]_{\Gamma_j} = 0, \tag{12}$$

$$[\phi]_{\Gamma_j} = 0. \tag{13}$$

Rewriting equation (4) as:

$$\boldsymbol{J} = \mu k T n \left\{ \nabla \left(\ln \frac{nT}{m^{3/2}} - \frac{q\phi + \chi}{kT} \right) + (q\phi + \chi) \nabla \left(\frac{1}{kT} \right) \right\}, \tag{14}$$

we impose the continuity of $\left(\ln \frac{nT}{m^{3/2}} - \frac{q\phi + \chi}{kT} \right)$, which leads to the following interface condition:

$$\left[m^{-3/2} n e^{-\frac{\chi}{kT}} \right]_{\Gamma_j} = 0. \tag{15}$$

As mentioned above, it would have been impossible to write $\boldsymbol{J}$ as (14) and to obtain condition (15) without the cancellation of the convective term in the momentum conservation equation.

We point out here that no physical assumptions were made to obtain the previous interface conditions: these conditions are derived from the equations and are necessary, from a mathematical point of view, to give sense to the

equations everywhere on Ω. From a physical point of view, they correspond to the continuity, at interfaces, of the normal component of the current density (condition (10)), of the normal component of the energy flux density (condition (10)), of the normal component of the electric displacement (condition (11)), of the electron temperature (condition (12)), of the scalar electric potential (condition (13)).

To complete our model, we need appropriate boundary conditions. On ohmic contacts, we assume charge neutrality and thermodynamic equilibrium. These assumptions lead to the conditions (see Selberherr, 1984):

$$n = N_d^+ \text{ on } \partial\Omega_O, \tag{16}$$

$$T = T_0 \text{ on } \partial\Omega_O, \tag{17}$$

$$\phi = \frac{kT_0}{q}\ln\left(\frac{N_d^+}{n_i}\right) + V \text{ on } \partial\Omega_O, \tag{18}$$

where V is the applied voltage and n_i the intrinsic carrier density.

The situation is different on Schottky contacts, where a potential barrier between the metal and the semiconductor exists (see Rhoderick and Williams, 1988). Applying the diffusion theory to describe the behaviour of such a contact, we obtain the following condition on the electron density:

$$n = N_c e^{-\frac{E_b}{kT_0}} \text{ on } \partial\Omega_S, \tag{19}$$

where N_c is the effective density of states in the conduction band and E_b the above-mentioned Schottky barrier. In practice, $\frac{E_b}{kT_0}$ is of order 10, so that the condition (19) implies the presence of a depletion region below the contact. Assuming thermal equilibrium at the contact, the condition for the electron temperature is:

$$T = T_0 \text{ on } \partial\Omega_S. \tag{20}$$

The condition for the electric potential is the one used in Technology Modeling Associates (1994):

$$\phi = \frac{E_g}{2q} + \frac{kT_0}{2q}\ln\left(\frac{N_c}{N_v}\right) + V - \frac{E_b}{q}, \tag{21}$$

where E_g is the energy gap between the valence band and the conduction band, and N_v the effective density of states in the valence band. Using the definition of n_i:

$$n_i = \sqrt{N_c N_v} e^{-\frac{E_g}{2kT_0}}, \tag{22}$$

we rewrite this expression as:

$$\phi = \frac{kT_0}{q}\ln\left(\frac{N_c}{n_i}\right) + V - \frac{E_b}{q} \text{ on } \partial\Omega_S. \tag{23}$$

When N_d^+ is close to N_c, condition (23) is similar to condition (18) in which the Schottky potential $\frac{E_b}{q}$ is subtracted to take into account the nature of the contact.

On the remaining part of the boundary, we assume insulating conditions (see Selberherr, 1984):

$$\frac{\partial n}{\partial \nu} = 0 \text{ on } \partial\Omega_N, \tag{24}$$

$$\frac{\partial T}{\partial \nu} = 0 \text{ on } \partial\Omega_N, \tag{25}$$

$$\frac{\partial \phi}{\partial \nu} = 0 \text{ on } \partial\Omega_N. \tag{26}$$

Equations (4) to (8), interface conditions (9) to (13), (15) and boundary conditions (16) to (20), (23) to (26) make up our stationary 3D energy-transport model for heterostructure devices. The corresponding drift-diffusion model is obtained by suppressing the energy conservation equation (6), (7) and setting $T = T_0$ everywhere in the above-mentioned energy-transport model. Our model is a generalization of the simplified hydrodynamic model (SHDM) of Apanovich *et al.* (1993), in the sense that it is applicable to semiconductor heterostructures and that it takes into account the variations of the electron effective mass through the $\nabla \ln m$ term in equation (4). The drift related part of the electron energy, which is included in the equations through the term $\frac{|\boldsymbol{J}|^2}{n^2}$, is neglected in the simplified hydrodynamic model of Apanovich *et al.,* (1993).

Physical parameters

To perform realistic simulations of electron devices, it is essential to model appropriately the physical parameters appearing in equations (4) to (8). Models based on theoretical considerations only are seldom sufficient and have to be replaced or completed by phenomenological ones. We present here models for the relevant physical parameters in gallium arsenide.

Electron affinity

The electron affinity in $Al_XGa_{1-X}As$ is given by (see Wang, 1989):

$$\chi(X) = 4.07 - \delta \cdot 1.247X \text{ eV}, \tag{27}$$

where X is the mole fraction of AlAs in GaAs ($X < 0.45$) and δ a factor representing the percentage of the gap energy found in the conduction band discontinuity ($\delta = 0.85$ or 0.6 according to the literature).

Electron effective mass

Assuming that most electrons belong to the Γ valley of the conduction band of GaAs and that this valley is parabolic, the electron effective mass in $Al_XGa_{1-X}As$ is a scalar given by (see Wang, 1989):

$$m(X) = (0.067 + 0.083X)m_e, \tag{28}$$

where $m_e = 9.109389 \cdot 10^{-31}$kg is the mass of the electron at rest.

Semiconductor dielectric constant

The dielectric constant of $Al_XGa_{1-X}As$ is (see Wang, 1989):

$$\epsilon(X) = (13.1 - 3.0X)\epsilon_0, \tag{29}$$

where $\epsilon_0 = 8.854187817 \cdot 10^{-12}$ $\mathrm{Asm^{-1}V^{-1}}$ is the vacuum permittivity.

Ionized donor density

We assume that each donor atom is singly ionized, so that:

$$N_d^+ = N_d, \tag{30}$$

where N_d is the density of donor atoms implanted by doping in the semiconductor.

Electron mobility

From a general point of view, the electron mobility in a semiconductor depends on each type of interaction between the electrons and the crystal lattice. As experimental data are lacking, we define a constant average mobility μ_0, called low-field mobility, which takes into account all interactions in a global way. This mobility also depends on the doping and is given by:

$$\mu_0 = \begin{cases} 8500\mathrm{cm}^2 s^{-1} V^{-1} \text{ in unintentionally doped GaAs,} \\ 800\mathrm{cm}^2 s^{-1} V^{-1} \text{in } \mathrm{Al}_X\mathrm{Ga}_{1-X}\mathrm{As} \text{ doped at } 10^{18}\mathrm{cm}^{-3} \end{cases}. \tag{31}$$

The expression of the mobility given in (31) is valid only for low electric fields. If they are higher that several $\mathrm{kVcm^{-1}}$, one has to take into account the electron velocity saturation phenomenon in the model. This is achieved by defining a field dependent mobility that reproduces correctly the electron velocity versus electric field curve in GaAs, and especially the negative differential mobility caused by the Γ valley to L valley electron transfer. We therefore use the following phenomenological model, known as Laux-Lomax model (see Selberherr, 1984):

$$\mu(E) = \frac{\mu_0 + v_{sat} \frac{E^3}{E_{crit}^4}}{1 + \left(\frac{E}{E_{crit}}\right)^4}, \tag{32}$$

where μ_0 is the low field mobility given in (31), $v_{sat} = 10^7 \text{cms}^{-1}$ the saturation velocity of electrons, $E_{crit} = 4 \cdot 10^3$ Vcm^{-1} a critical electric field and E the electric field intensity.

Energy relaxation time

We use a constant average energy relaxation time τ_w whose value is (see Wang and Hsieh, 1990):

$$\tau_w = 1 \text{ ps}. \tag{33}$$

Electron thermal conductivity

We model the electron thermal conductivity with a generalized Wiedemann-Franz law:

$$\kappa = \delta \frac{k^2}{q} \mu n T, \tag{34}$$

where, according to Wang and Hsieh (1990), $\delta = \frac{5}{2}$.

Numerical methods

As mentioned above, the natural unknowns of our energy-transport model are the electron density n, the electron temperature T and the electrostatic potential ϕ. The unknown n is not continuous at the interface between two different semiconductors and therefore not suitable for writing a weak formulation of the model. We replace this unknown by a new one, ξ, similar to a quasi-Fermi potential and defined by:

$$n(\xi, T, \phi) = \frac{m^{3/2}}{T} e^{\xi + \frac{q\phi + \chi}{kT}}. \tag{35}$$

As can be inferred from condition (15), ξ is continuous at interfaces. Moreover, the positivity of n is ensured by the change of unknown (35) as long as T is positive. So, we replace n by ξ in the system (4) to (8) and define the following functional spaces:

$$\begin{aligned} V &= H_{0,N}(\text{div}; \Omega) \\ &= \left\{ v \in L^2(\Omega) | \nabla \cdot v \in L^2(\Omega), v \cdot \nu = 0 \text{ on } \partial\Omega_N \right\}, \end{aligned} \tag{36}$$

$$W = L^2(\Omega), \tag{37}$$

$$X_f = \left\{ x \in H^1(\Omega) | x = f \text{ on } \partial\Omega_D \right\}. \tag{38}$$

We multiply equations (4), (5), (7) and (8) (in the ξ formulation) by appropriate test functions in the above spaces and integrate them over Ω, taking into account interface conditions (9) to (13), (15). We get the following weak mixed formulation:

Problem 1. Find $(\boldsymbol{J}, \xi, T, \phi) \in V \times W \times X_{T_0} \times X_{\phi_0}$ such as $\forall(\tilde{\boldsymbol{J}}, \tilde{\xi}, \tilde{T}, \tilde{\phi}) \in V \times W \times X_0 \times X_0$:

$$\int_\Omega \frac{1}{km^3/^2\mu} e^{-\xi-\frac{q\phi+\chi}{kT}} \boldsymbol{J} \cdot \tilde{\boldsymbol{J}} dx + \int_\Omega \xi \nabla \cdot \tilde{\boldsymbol{J}} dx + \int_\Omega \frac{q\phi+\chi}{kT} \nabla \ln T \cdot \tilde{\boldsymbol{J}} dx = \int_{\partial\Omega_D} \xi_0 \tilde{\boldsymbol{J}} \cdot \nu ds, \tag{39}$$

$$\int_\Omega \tilde{\xi} \nabla \cdot \boldsymbol{J} dx = 0, \tag{40}$$

$$\begin{aligned} &\int_\Omega qk\nabla T \cdot \nabla \tilde{T} dx \\ &+ \int_\Omega \left(\frac{5}{2} kT + \frac{m}{2q^2} \frac{|\boldsymbol{J}|^2}{n^2(\xi, T, \phi)} - (q\phi + \chi) \right) \boldsymbol{J} \cdot \nabla \tilde{T} dx \\ &= \int_\Omega -\frac{qn(\xi, T, \phi)}{T_w} \left(\frac{m}{2q^2} \frac{|\boldsymbol{J}|^2}{n^2(\xi, T, \phi)} + \frac{3}{2} k(T - T_0) \right) \tilde{T} dx, \end{aligned} \tag{41}$$

$$\int_\Omega \epsilon \nabla \phi \cdot \nabla \tilde{\phi} dx = \int_\Omega q(N_d^+ - n(\xi, T, \phi)) \tilde{\phi} dx. \tag{42}$$

In Problem 1, the functions $\xi_0 = Tr(\xi)$, $T_0 = Tr(T)$, $\phi = Tr(\phi)$: $\partial\Omega_O \bigcup \partial\Omega_S \rightarrow R$ are the boundary values for the unknowns ξ, T, ϕ, given by the conditions (16) to (20), (23).

Before writing a numerical algorithm to solve Problem 1, we introduce a fully decoupled version of the equations (39) to (42):

Problem 2 (Current continuity equation). Let $(\hat{T}, \hat{\phi}) \in X_{T_0} \times X_{\phi_0}$ be given functions. Find $(\boldsymbol{J}, \xi) \in V \times W$ such as $\forall(\tilde{\boldsymbol{J}}, \tilde{\xi}) \in V \times W$:

$$\int_\Omega \frac{1}{km^{3/2}\mu} e^{-\xi-\frac{q\hat{\phi}+\chi}{kT}} \boldsymbol{J} \cdot \tilde{\boldsymbol{J}} dx + \int_\Omega \xi \nabla \cdot \tilde{\boldsymbol{J}} dx = -\int_\Omega \frac{q\hat{\phi}+\chi}{k\hat{T}} \nabla \ln \hat{T} \cdot \tilde{\boldsymbol{J}} dx + \int_{\partial\Omega_D} \xi_0 \tilde{\boldsymbol{J}} \cdot \nu ds, \tag{43}$$

$$\int_\Omega \tilde{\xi} \nabla \cdot \boldsymbol{J} dx = 0. \tag{44}$$

Problem 3 (Poisson equation). Let $(\hat{\xi}, \hat{T}) \in W \times X_{T_0}$ be given functions. Find $\phi \in X_{\phi_0}$ such as $\forall \tilde{\phi} \in X_0$:

$$\int_\Omega \epsilon \nabla \phi \cdot \nabla \tilde{\phi} dx = \int_\Omega q\Big(N_d^+ - n(\hat{\xi}, \hat{T}, \phi)\Big)\tilde{\phi} dx. \tag{45}$$

Problem 4 (Energy conservation equation). Let $(\hat{\boldsymbol{J}}, \hat{\xi}, \hat{T}, \hat{\phi}) \in V \times W \times X_{T_0} \times X_{\phi_0}$ be given functions. Find $T \in X_{T_0}$ such as $\forall \tilde{T} \in X_0$:

$$\begin{aligned} &\int_\Omega q\kappa \nabla T \cdot \nabla \tilde{T} dx \\ &+ \int_\Omega \left(\frac{5}{2}kT + \frac{m}{2q^2}\frac{|\hat{\boldsymbol{J}}|^2}{n^2(\hat{\xi}, \hat{T}, \hat{\phi})} - (q\hat{\phi} + \chi)\right)\hat{\boldsymbol{J}} \cdot \nabla \tilde{T} dx \\ &= \int_\Omega -\frac{qn(\hat{\xi}, \hat{T}, \hat{\phi})}{\tau_w}\left(\frac{m}{2q^2}\frac{|\hat{\boldsymbol{J}}|^2}{n^2(\hat{\xi}, \hat{T}, \hat{\phi})} + \frac{3}{2}k(T - T_0)\right)\tilde{T} dx. \end{aligned} \tag{46}$$

The numerical solution of the model is obtained with the help of the following algorithm:

Algorithm 1. Let $m, n \in N$ be iteration indexes, $\|.\|$ an adequate norm, ω a relaxation factor and $\varepsilon_{\text{decoupling}} > 0$ a threshold level. The following steps are performed:

(1) Build an initial approximation $(T^{(0)}, \phi^{(0,0)})$. Let $m = n = 1$.

(2) For $(\hat{T}, \hat{\phi}) = (T^{(m-1)}, \phi^{(m-1,n-1)})$, compute $(\boldsymbol{J}^{(m-1,n)}, \xi^{(m-1,n)})$ solution of Problem 2.

(3) For $(\hat{\xi}, \hat{T}) = (\xi^{(m-1,n)}, T^{(m-1)})$, compute $\phi^{(m-1,n)}$ solution of Problem 3.

(4) Calculate:

$$\varepsilon = \max\left(\frac{\|\xi^{(m-1,n)} - \xi^{(m-1,n-1)}\|}{\|\xi^{(m-1,n)}\|}, \frac{\|\phi^{(m-1,n)} - \phi^{(m-1,n-1)}\|}{\|\phi^{(m-1,n)}\|}\right).$$

(5) If $\varepsilon \geq \varepsilon$ decoupling, let $n := n + 1$; go to 2.

(6) Let $(\boldsymbol{J}^{(m,0)}, \xi^{(m,0)}, \phi^{(m,0)}) = (\boldsymbol{J}^{(m-1,n)}, \xi^{(m-1,n)}, \phi^{(m-1,n)})$.

(7) For $(\hat{\boldsymbol{J}}, \hat{\xi}, \hat{T}, \hat{\phi}) = (\boldsymbol{J}^{(m,0)}, \xi^{(m,0)}, T^{(m-1)}, \phi^{(m,0)})$, compute $T^{(m)}$ solution of Problem 4.

(8) Let $T^{(m)} := \omega T^{(m)} + (1 - \omega)T^{(m-1)}$.

(9) Calculate:

$$\varepsilon = \frac{\|T^{(m)} - T^{(m-1)}\|}{\|T^{(m)}\|}.$$

(10) If $\varepsilon \geq \varepsilon$ decoupling, let $m := m + 1$, $n = 1$; go to 2.

(11) The solution of Problem 1 is $(\boldsymbol{J}^{(m,0)}, \xi^{(m,0)}, T^{(m)}, \phi^{(m,0)})$.

From a practical point of view, the algorithm 1 is applied to a discretized version of Problems 2 to 4.

The discretization of the current continuity equation is realized by means of the mixed Raviart-Thomas RT_0 elements with interelement Lagrange multipliers (see Brezzi *et al.,* 1988) for a detailed description of the method). The nonlinear system arising from the discretization of Problem 2 is solved using a Newton method. At each iteration of this method, a banded, symmetric, positive definite matrix is obtained.

As the Poisson equation (Problem 3) is non-linear in ϕ, we linearize it with a pseudo-Newton method. The discretization of the arising linear equation is no problem and thus carried out by a standard P_1 finite element method. The corresponding linear system is banded, symmetric and positive definite.

The energy conservation equation (4) is a convection-diffusion problem. When the convective term is dominant, it is well known that the standard finite element methods give poor approximations of the solution. To get rid of this problem, we discretize equation (46) using P_1 finite elements with streamline diffusion (see Johnson, 1987). We obtain a linear system characterized by a non-symmetric band matrix.

It is important to note here that the formulation of the problem with the unknowns (ξ, T, ϕ) is not adequate for the drift-diffusion model. It is indeed better to replace the unknown ξ by $\rho = e^{\xi}$: ρ is continuous at interfaces and the arising current continuity equation is linear in ρ, which is not the case with the unknown ξ. The linearization of the current continuity equation mentioned above is therefore useless, so that the corresponding numerical algorithm for the drift-diffusion model is significantly faster in the (ρ, T, ϕ) formulation than in the (ξ, T, ϕ) formulation. The drawback of the latter formulation is the fact that it does not work well with the hydrodynamic model, essentially because the positivity of ρ, and thus the positivity of n, is not implicit in the change of unknown:

$$n(\rho, T, \phi) = n(e^{\xi}, T, \phi) = \rho \frac{m^{3/2}}{T} e^{\frac{q\phi + \chi}{kT}}, \tag{47}$$

where T is assumed to be positive.

Concerning the convergence properties of our algorithm, we can say that the number of global iterations required to obtain the numerical solution largely depends on the initial approximation, on the mesh and on the decoupling threshold. In practical cases with relatively fine meshes (about 5,000 triangles) and $\varepsilon_{\text{decoupling}} \approx 10^{-6}$, this number varies from three to more than 50. Thus, the CPU time needed to compute the solution for one applied voltage (V_{gs} and V_{ds} fixed) ranges between 0.5 and ten minutes on a Silicon Graphics workstation powered by a MIPS R10000 processor. As a result, the calculation of a $I_d(V_{ds})$ curve with typically 100 bias points takes about five hours.

Application

To validate the model and the numerical methods presented in the previous sections, we simulate a real AlGaAs/GaAs modulation doped field effect transistor (MODFET). This device, referred to by IMO S433 MODFET, was produced and measured at the Institut de micro- et optoélectronique in the Département de physique of the Ecole polytechnique fédérale de Lausanne. The geometry of the device is given in Figure 2 and its structural properties in Table I. To give an insight to the results that can be obtained with our program, we present in Figure 3 plots of some important physical quantities computed for a gate-source voltage $V_{gs} = -1$V and a drain-source voltage $V_{ds} = 1.8$V. The top plot shows the current density $\boldsymbol{J}$ ([Am^{-2}]) in the transistor. As could be awaited, current flows from the drain to the source, passing by the depletion zone below the gate contact. An important part of the current flows through the two-dimensional electron gas. The electron

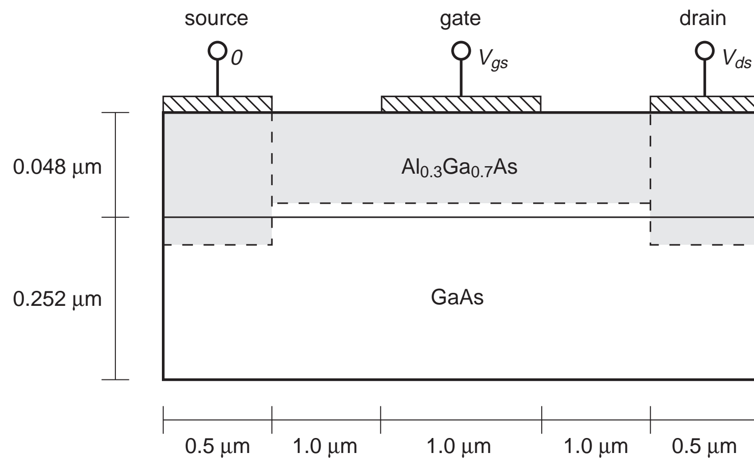

Figure 2.
Geometry of IMO S433 MODFET

Table I.
Structural properties of IMO S433 MODFET

Parameter	Unit	AlGaAs active zone	AlGaAs spacer	GaAs
thickness	[μm]	0.040	0.008	0.252
X	[ ]	0.3	0.3	0.0
N_d	[cm^{-3}]	$1.5 \cdot 10^{18}$	10^{15}	10^{15}
T_0	[K]		300	
V_d	[V]		0.8	

temperature ([K]) is given in the left bottom plot. The effect of electron heating is clearly visible and happens mainly in the spacer layer, between the drain end of the gate and the right border of the drain. This heating zone corresponds to the region where the electric field is the most intense. This observation shows that the dominant source term in the energy conservation equation (7) is the Joule term $-\boldsymbol{J} \cdot \nabla\left(\phi + \frac{\chi}{q}\right)$. The right bottom plot depicts the electric potential ([V]) in the device. Influence of the contacts and high field regions are visible on the plot. From a physical point of view, the results shown in Figure 3 are correct. We tried to compare them to the ones calculated with the commercial simulation software TMA MEDICI (see Technology Modeling Associates, 1994), with a model as close to ours as possible and with the same discretization mesh. Up to the voltages where the algorithm was used in MEDICI converges (some tenths of volt for this particular device), the results obtained are qualitatively the same.

For electrical engineers, one of the most important features of the transistor are the drain current I_d versus drain voltage V_{ds} characteristics. In Figure 4,

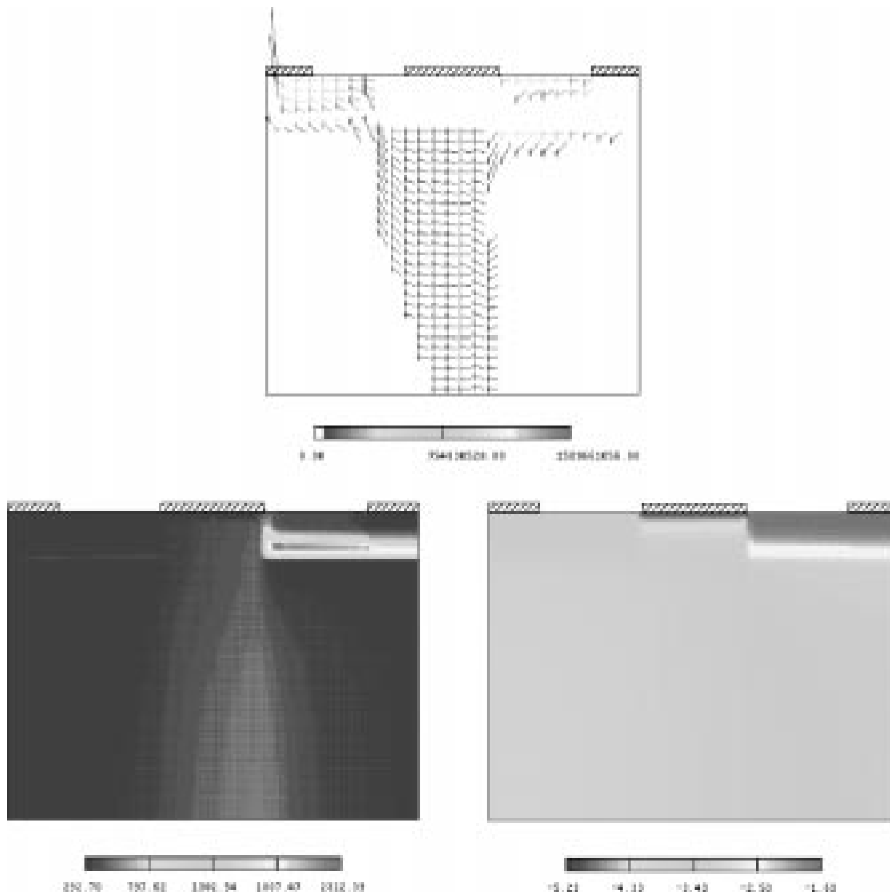

Figure 3.
Current density, electron temperature and electric potential in IMO S433 MODFET ($V_{gs} = -1$V, $V_{ds} = 1.8$V)

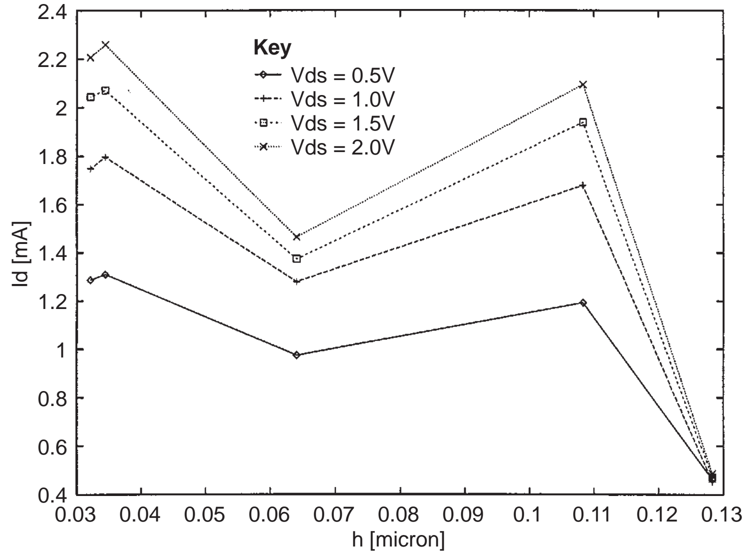

Figure 4.
Convergence of the drain current with the mesh parameter for different drain voltages (V_gs = 0.0V)

we show that the drain current computed with our algorithm converges to the theoretical one when the mesh parameter h tends to 0. To realize the figure, we used five non-isotropic meshes characterized by parameters ranging from 0.0321μm to 0.1283μm. As one can see, a mesh with a relatively large parameter (h = 0.1083μm) but refined near the interface leads to a better drain current than the one obtained with a fine mesh (h = 0.0641μm) not sufficiently refined near the junction. The convergence property verified above, which is essential to give sense to the calculated quantities, is seldom mentioned in the literature.

The linear part of the $I_d(V_{ds})$ characteristic for $V_{gs} = 0.0$V is represented in Figure 5. The solid line corresponds to the experimental measurements, the long-dotted one was computed using the drift-diffusion model and the short-dotted one with the energy-transport model. The difference between the calculated and measured characteristics are significant, but not dramatic. The reader should indeed keep in mind that no fitting or smoothing of the physical parameters was done to perform the simulation: the models for the physical parameters are those described above. In addition, the heavy doping zone below ohmic contacts was not taken into account in the simulation. As the main effect of this zone is to decrease contact resistance, we understand that the slope of the computed current-voltage curves is less than that of the measured ones. In Figure 5, we observe that the drift-diffusion model gives a higher current than the energy transport model. This result is apparently in contradiction with the results obtained in Snowden and Loret (1987) for the case of MESFETs. This apparent contradiction shows clearly the influence of the model for the electron mobility and the energy relaxation time on the computed results: the authors of Snowden and Loret (1987) use an energy-

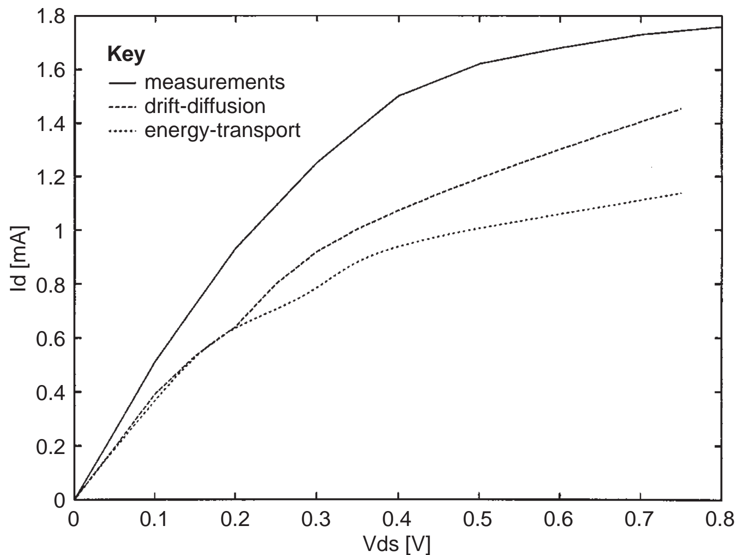

Figure 5.
Drain current versus drain voltage characteristic ($V_{gs} = 0.0V$)

dependent mobility and relaxation time, both obtained by Monte-Carlo simulation, whereas we employ a field dependent mobility and a constant relaxation time. The sensitivity of the model to these physical parameters is therefore important. The question of deciding what are the best mobility and relaxation time models cannot be answered simply and should be investigated on several different real devices.

References

Apanovich, Y., Lyumkis, E., Polski, B., Shur, A. and Blakey, P. (1993), "A comparison of energy balance and simplified hydrodynamic models for GaAs simulation", *COMPEL,* Vol. 12 No. 4, pp. 221-30.

Baccarani, G. and Wordeman, M.R. (1985), "An investigation of steady-state velocity overshoot in silicon", *Solid-State Electronics,* Vol. 28 No. 4, pp. 407-16.

Brezzi, F., Marini, L.D. and Pietra, P. (1988), *Numerical Simulation of Semiconductor Devices,* Istituto di Analisi Numerica del Consiglio Nazionale delle Ricerche, No. 608, Pavia, Italy.

Cercignani, C. (1990), *Mathematical Methods in Kinetic Theory,* Plenum Press, New York, NY.

El Boukili, A. (1995), "Analyse mathématique et simulation numérique bidimensionnelle des équations des semi-conducteurs par l'approche éléments finis mixtes", Ph.D. thesis, Université Pierre & Marie Curie, Paris VI.

Feng, Y. and Hintz, A. (1988), "Simulation of submicrometer GaAs MESFETs using a full dynamic transport model", *IEEE Transactions on Electron Devices,* Vol. 35 No. 9, pp. 1419-31.

Forghieri, A., Guerrieri, R., Ciampolini, P., Gnudi, A., Rudan, M. and Baccarani, G. (1988), "A new discretization strategy of the semiconductor equations comprising momentum and energy balance", *IEEE Transactions on Computer-Aided Design,* Vol. 7 No. 2, pp. 231-42.

Johnson, C. (1987), *Numerical Solution of Partial Differential Equations by the Finite Element Method,* Cambridge University Press, New York, NY.

Lab, C. (1997), "Modélisation et simulation numérique de dispositifs à hétérostructures semi-conductrices: application aux MODFETs AlGaAs/GaAs", Thèse, Ecole Polytechnique Fédérale de Lausanne, Lausanne.

Markovich, P.A., Ringhofer, C.A. and Schmeiser, C. (1991), *Semiconductor Equations*, Springer-Verlag, Wien.

Marshak, A.H. and van Vliet, K.M. (1984), "Electrical current and carrier density in degenerate materials with nonuniform band structure", *Proceedings of the IEEE,* Vol. 72, pp. 148-64.

Poupaud, F. and Yamnahakki, A. (1990), "Drift diffusion models for heterostructures in semiconductors", in Marcati, Markovich and Natalini (Eds), *Mathematical Problems in Semiconductor Physics,* Longman.

Rhoderick, E.H. and Williams, R.H. (1988), *Metal-Semiconductor Contacts,* Clarendon Press, Oxford.

Selberherr, S. (1984), *Analysis and Simulation of Semiconductor Devices,* Springer-Verlag, Wien.

Shawki, T. (1990), "Conception d'un modèle hydrodynamique bidimensionnel de transistors à effet de champ à hétérostructure: application à l'analyse physique et à l'optimisation des composants submicroniques", Université des Sciences et Techniques de Lille-Flandres-Artois.

SILVACO International (1995), *ATLAS, Device Simulation Software,* SILVACO International, Santa Clara, CA.

Snowden, C.M. and Loret, D. (1987), "Two-dimensional hot-electron models for short-gate-length GaAs MESFETs", *IEEE Transactions on Electron Devices,* Vol. ED-34 No. 2, pp. 212-23.

Technology Modeling Associates (1994), *MEDICI, Two-Dimensional Device Simulation Program,* Technology Modeling Associates, Inc., Palo Alto, CA.

Wang, S. (1989), *Fundamentals of Semiconductor Theory and Device Physics,* Prentice-Hall, Inc., Englewood Cliffs, NJ.

Wang, T. and Hsieh, C.-H. (1990), "Numerical analysis of nonequilibrium electron transport in AlGaAs/InGaAs/GaAs pseudomorphic MODFETs", *IEEE Transactions on Electron Devices,* Vol. 37 No. 9, pp. 1930-8.